

Ent-Kaurane diterpenoid glycosides as soft-templates for the synthesis of high-surface area anatase titanium dioxide. An electron microscopy study and Rietveld Refinement

Ángela B. Sifontes^{1,*}, Edward E. Ávila^{1,**}, Edgar Cañizales², Wendy Rondón¹, Brenda Gutiérrez¹, Franklin J. Méndez¹, Andrea Mónaco¹, Andreina Yáñez¹, Yraida Díaz¹, Joaquín L. Brito¹

¹ Centro de Química, Instituto Venezolano de Investigaciones Científicas (IVIC), Apartado 20632, Caracas 1020-A Venezuela

² Área de Análisis Químico Inorgánico. PDVSA. INTEVEP. Los Teques 1070-A, Venezuela

*corresponding author e-mail address: angelasifontes@gmail.com

**corresponding author e-mail address: edebavso@gmail.com

ABSTRACT

In the present study, high-resolution transmission electron microscopy (HRTEM) and field emission scanning electron microscopy (FE-SEM) were used to investigate the effect of *ent-Kaurane diterpenoid glycoside* molecules as soft templates on the synthesis of anatase titanium dioxide. Such studies revealed that the supramolecular arrangement that form the *ent-Kaurane diterpenoid* serve as mold, around which a framework is built up. The images TEM and HRTEM obtained suggested that the synthesized anatase titanium dioxide contain structures consisting of aggregates of nanoparticles with an average diameter of about 3-8 nm. These observations support that the formation of porous nanostructured anatase arises as a consequence of the removal of the organic molecules. In this work, the chemical modification of titanium alkoxide in the aqueous system is also discussed. Additionally, the nanomaterial was characterized by powder X-ray diffraction data (Rietveld refinement), and N₂ adsorption porosimetry.

Keywords: *Ent-Kaurane diterpenoid glycoside, Soft-template, High-Resolution Transmission Electron Microscopy, Rietveld Refinement.*

1. INTRODUCTION

Currently, the oxide of titanium (TiO₂) is considered to be a material of great technological importance due to its photoconductive and photocatalytic properties, demonstrating efficiency in the degradation of azo-dyes, oxidation of volatile organic compounds and degradation of organic compounds, chlorinated, among others [1]. Today, many investigations are aimed to improve the physicochemical properties and catalytic activity of titanium oxide. The efficiency of these materials is closely related to its crystalline structure and morphology. It is here where the synthesis method plays an important and decisive role [1, 2, 3, 4].

Titanium dioxide has three known polymorphs, rutile tetragonal ($a = 4.5937 \text{ \AA}$, $c = 2.9587 \text{ \AA}$) ($P4_2/mmm$), anatase tetragonal ($a = 3.7845 \text{ \AA}$, $c = 9.5143 \text{ \AA}$) ($I4_1/amd$) and brookite orthorhombic ($Pcab$) ($a = 5.4558 \text{ \AA}$, $b = 9.1819 \text{ \AA}$, $c = 5.1429 \text{ \AA}$). Rutile is the most stable phase and anatase is most useful for photocatalysis and in solar energy applications possibly because its electron mobility is higher than that of rutile [4, 5, 6].

In most potential applications, the size and the structure of the particles play a significant role in deciding their functions [4, 5]. Particularly, materials at nanometer scale have been extensively studied during the last decades due to their unique properties and a whole range of applications. In this sense, various synthesis methodologies have been formulated to obtain TiO₂ on the nanoscale [7]. Physical and chemical vapor deposition, sol-gel, hydrothermal, electrotemplating and solvothermal methods among others have been extensively used as synthetic routes [8-10]. However, there always has been a constant effort to decrease the cost

incurred in the manufacturing of the nanomaterials to make them more feasible for industrial production.

A generally applied synthesis strategy for this kind of materials is the soft-templating method. Soft-templating is defined as a process in which organic molecules or supramolecular aggregates serve as a 'mold' around which a framework is built up [11]. The removal of these organic molecules results in a cavity that retains the same morphology and structure of the organic molecules. Soft-templating is versatile, but it is also a complicated synthesis method in which hydrolysis and condensation reactions around micelles of the template result in the formation of an amorphous network of titanium dioxide [12]. This is followed by a thermal treatment to remove the template and crystallize the TiO₂. The disadvantage of this procedure is the use of high thermal treatment temperatures, necessary to create the photocatalytically active anatase crystal phase, which causes the collapse of the porous structure due to thermal instability of the organic soft template [12-14].

On the other hand, the obtained meso-structures from the self-assembly process are very dependent on temperature, solvent, concentration, hydrophobic/hydrophilic properties, interface interaction, ionic strength and many other parameters [12]. In this sense, block copolymers, anionic surfactants, cationic surfactants, and primary amines have been developed to prepare crystalline TiO₂ with well-defined mesopores structures [8].

Recently, the aqueous extract of *Stevia rebaudiana bertonii* has been used for the preparation of metallic nanoparticles and nanostructured oxides (Figure 1) [15]. The extraction and

purification of steviol glycosides, constituents of *Stevia rebaudiana* (native plant to certain regions of Paraguay and Brazil), allows the preparation of a synthesis media rich in molecular structures such as *Rebaudioside A*, *Rebaudioside B*, *Rebaudioside C*, *Rebaudioside D*, *Rebaudioside E*, *Rebaudioside F*, *Ruboside*, *Esteviol bioside*, *Dulcoside A* and *Steviol monoside* (Figures 2,3) [15].

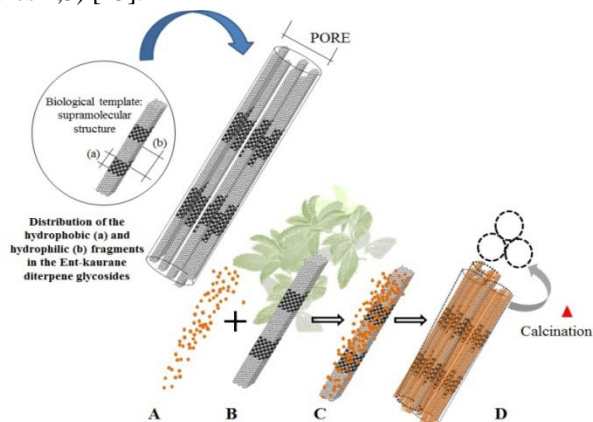


Figure 1. Mechanism proposed for the synthesis of materials using the kaurane diterpenoids as biological templates. A) Metal alkoxide solution, B) supramolecular structures in *Stevia rebaudiana* aqueous extract leaf, C) template and inorganic precursor and D) building of porous structures.

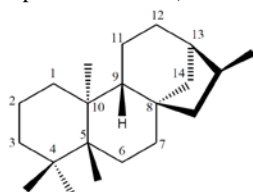


Figure 2. Ent-Kauranediterpenoid molecule.

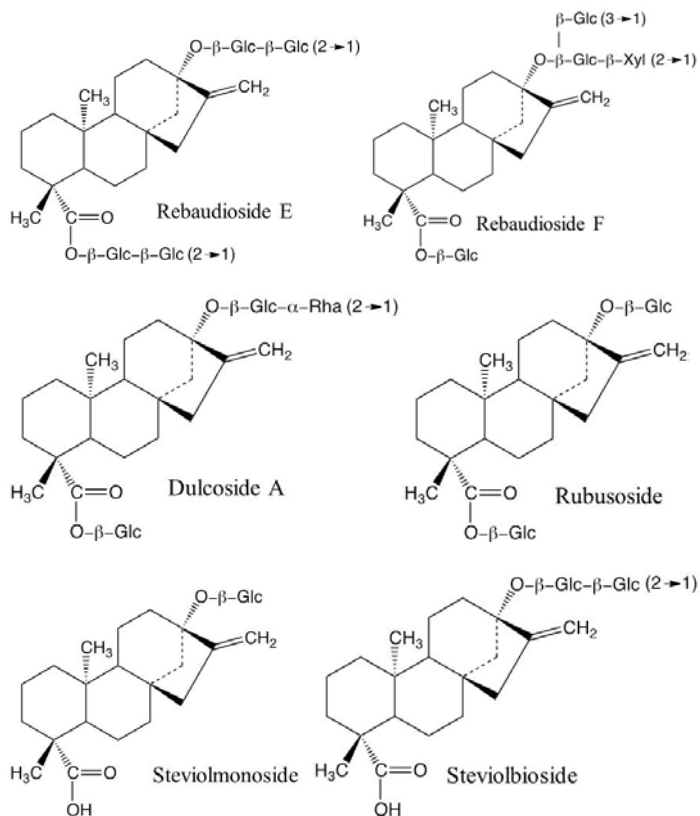
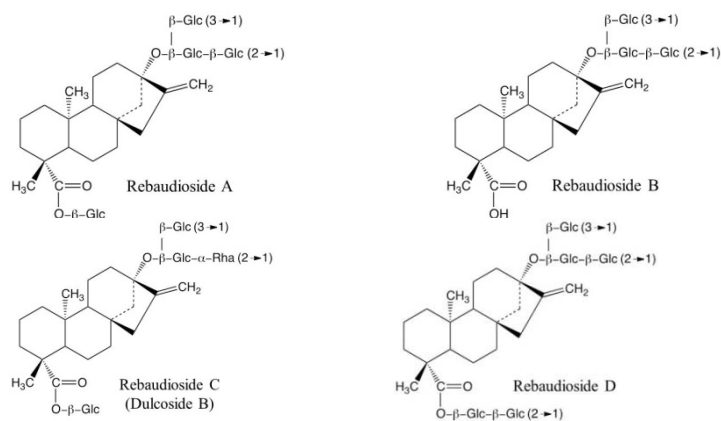


Figure 3. Ent-Kauranediterpenoid molecules from *S. rebaudiana* aqueous extract.

The supramolecular structures former by this ent-Kaurane diterpenoid molecules are employed in soft-template method to obtain a nanometric mesoporous anatase (Figure 1), highly crystalline, avoiding the disadvantages which usually are presented with the use of surfactants molecules. In the soft template approach, the control of the size and mechanical stability of the supramolecular structures could become a problem. Therefore, a new protocol using biological materials through which the structure can be made easily is of great interesting.

In the present study, we focused on HRTEM and FE-SEM characterization of TiO₂ nanopowders produced by biosynthesis, employing the supramolecular self-assembly of diterpene glycosides as a soft-template patterning. In addition, a discussion about the chemical modification of titanium alkoxide in this aqueous system has been added.

2. EXPERIMENTAL SECTION

2.1. Preparation of the *S. rebaudiana* leaf extract.

Portions of 1.20 g of leaves of *S. rebaudiana* were extracted with 50 mL of hot water (65 °C) for 3 h, as described previously by Nishiyama *et al.* [16]. The crude extract was filtered through a Whatman qualitative filter paper No. 1.

2.2. Synthesis of nanometric TiO₂.

Synthesis of nanometric titania was carried out from aqueous solutions employing titanium isopropoxide (Sigma-Aldrich) as a metal precursor and *S. rebaudiana* leaf extract as a

soft-template. In a typical preparation, 5.84 g of titanium isopropoxide was dissolved in 54 mL of distilled water. The resultant solution was magnetically stirred at room temperature for 2 h. Subsequently, the extract was added dropwise. The pH value was adjusted to 5 using a diluted acid nitric aqueous solution. The obtained solution was evaporated and dried at 80 °C for 48 h. Finally, the resulting solid was calcined to remove the template. This was carried out in a tubular furnace under air atmosphere, with a heating rate of 5 °C/min up to 500 °C, and kept at the maximum temperature for 6 h.

2.3. Characterization and instrumentation

X-ray Diffraction (XRD) pattern data of TiO₂ was collected on a Panalytical diffractometer, model X'Pert Pro, and CuK α radiation in the 2 θ range between 5-80°, operating at 40kV and 20 mA. Phase identification performed using the MATCH! 2 program (version 2.3.3, Build 434) Crystal Impact, coupled with the Release 2011 PDF-2 database. The Rietveld refinement performed with the complete pattern and obtained a good agreement with the structures reported in both the PDF (code 00-071-1167) and the ICSD (code 172916), this last used as a model for the Rietveld refinement. The structure TiO₂ was refined with the Rietveld method [17] used the program Fullprof/Wfp2k (Rodriguez-Carvajal, 2014) using the graphical interface Winplotr (Roisnel& Rodriguez-Carvajal, 2014). The peak shapes modeled using the pseudo-Voigt function. Background modeled using the interpolation function with eight points. The isotropic atomic displacement parameters were refined as one overall U_{iso} for the non-oxygen atoms starting from a value of 0.05 Å². Nevertheless,

one constraint applied to U_{iso} for modeled of isotropic atomic displacement parameters of oxygen atom following riding-model.

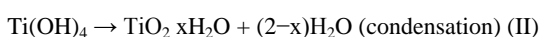
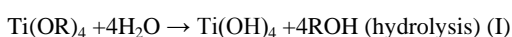
The mean grain size (D) of the prepared TiO₂ nanoparticles was calculated from X-ray line broadening of the listed reflections in the Table 1, using Scherrer's equation [10], (i.e. $D = K\lambda/(\beta \cos \theta)$), where λ is the wavelength of the X-ray radiation, K is a constant taken as 0.89, θ is the diffraction angle, β (rad) is the full-width at half-maximum (FWHM). The particle size was calculated using the Scherer's equation.

The morphologies of particles were observed by field emission scanning electron microscopy (FE-SEM), using a Quanta 250 FEG scanning electron microscope (accelerating voltage of 30 kV). The evaluation by transmission electron microscopy was performed on a TEM 1220 JEOL instrument operated at 100 kV and a JEOL JEM-2100 microscope with LaB₆ filament (accelerating voltage of 200 kV). The samples were prepared by suspending the powders in an ethanol-based liquid and pipetting the suspension onto a carbon/collodion coated.

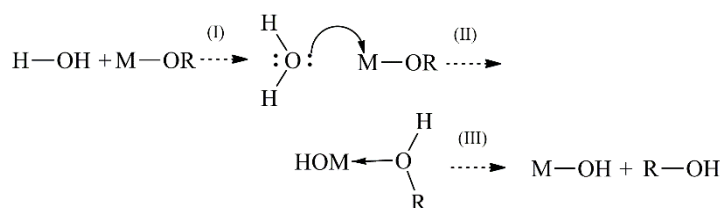
3. RESULTS SECTION

3.1. Synthesis mechanism.

In general, the hydrolysis and condensation of the titanium alkoxides are controlled mainly by two parameters: the concentration of starting reagents and the hydrolysis ratio (rw: H₂O/Ti). These two factors not only modify the speed of reactions, but also change the degree of hydrolysis of the complexes that form in the system. In this sense, it has been shown, that the size, stability and morphology of the sol generated is strongly affected by the molar ratio water/titanium (r:H₂O/Ti). Therefore, in the presence of water, the alkoxides are hydrolyzed and subsequently polymerized to form a three-dimensional network of oxide [18, 19]. These reactions can be described in the following way:



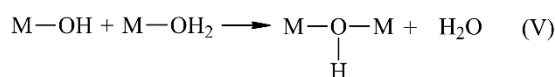
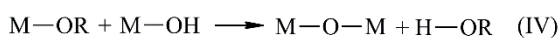
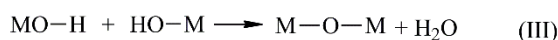
The hydrolysis of the alkoxide (I) is made by adding water, generating a hydroxo group reagent M–OH. In this regard, it has already been proposed a general three steps mechanism [18-21], as shown below:



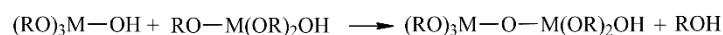
The first step corresponds to the nucleophilic addition of a water molecule to the metallic atom (Ti), leading to a transition state in which the number of coordination of the metal is increased in a unit. A second step occurs in the transfer of a proton from the water molecule next to –OR the adjacent group, negatively charged oxygen generating an intermediate species[18-21].

The third step is the leaving of the species –OR, which has more positive partial charge within the state of transition. Subsequently, it takes place the condensation, a complex process

that in these systems could be occurring through chemical reactions that have been described as: oxolation (III) alcoxolation (IV) and ololation (V), generating simultaneously during the course of the nucleation and crystallization, as shown below:



As mentioned in the literature, it is expected, for the metal alkoxides, that species hydrolyzed type M(OR)₃(OH) to condense via alcoxolation and not oxolation:



Generally, condensation results in the formation of oxo-alkoxides with different variations in their compositions Ti_xO_y.OR(4x–2y). It is important to mention, that the addition of mineral acids, such as HNO₃, in the aqueous medium, can increase the kinetics of the hydrolysis-condensation reactions and the structure of the condensed product. –OR groups can easily be protonated by ions H₃O⁺, consequently all –OR groups can be hydrolyzed, provided it has been added enough water. In the presence of H₃O⁺, condensation occurs between hydrolyzed species, quickly formed, ZX(OH) x M (OR) [5, 23].

Various factors in addition to the water/alkoxide ratio also affect the kinetics of network forming reactions[19]. Such factors include the type of alkyl groups in the alkoxide, the host medium, molecular separation of species, catalysts, and temperature [18, 19]. The molecular separation of species during the hydrolytic polycondensation by dilution was found to affect the densification rate as well as the crystallization of TiO₂ samples. As a result, depending on the experimental procedure, adjustment of pH and the number of water molecules present in the medium of synthesis,

it would lead that the precipitation of some phases of TiO₂ occurs preferentially [19-21]. This can be attributed to the order in which appear the competitive mechanisms of condensation, oxolation /alcoxolation (formation of oxygen by the removal of water or alcohol elimination bridges) and ololation (formation of bridges hydroxy by elimination of solvent molecules).

In particular, where the alcoxolation occurs before the ololation reaction, condensation may be leading to the formation of the typical chains in the anatase phase. For this purpose, "it is required that reaction occurs in an aqueous system" [18-21], so as the methodology used in this work.

On the other hand, the combination of an inorganic polymeric network with organic component or in this case, "a biological soft-template", leads to mixed of hybrid material composite by inorganic-organic polymers. In this compound, new bonds are formed, which could be used for modifying the network formers or could also form new structures, depending on the reactivity of the organic groups attached to the biomolecules. However, it has been mentioned that is not possible this modifications in the case of transition metal oxide gels, presumably because the ionic M-C bonds upon hydrolysis are destroyed. Differently, the organic modification could be achieved with polymerizable ligands or use of compounds that appear to react with metal alkoxide giving the corresponding mixed alkoxide derivatives [22]. In this sense, it is known that metal alkoxides could be reacted with a variety of chemical compounds containing nucleophilic hydroxyl groups and the chemical modification can be performed leading to new molecular precursors that exhibit a wide range of new properties [22]. Generally, the substitution reaction could occur when highly electrophilic metal alkoxides react with nucleophilic hydroxylated ligands. Therefore, alkoxy groups are then replaced by new ligands, which can be removed upon hydrolysis [18-22], in this case a metal oxide is obtained. On the other hand, a mixed organic-inorganic network is formed when the metal-ligand bond cannot be broken upon hydrolysis. These "modifiers" should be removed during the condensation reactions promoting the formation of polymeric gel. Consequently, this molecular modification has a strong effect on parameters such as: gelation time, particle morphology and porosity. Thus, the relative hydrolysis and condensation rates are modified and different products can be obtained. Additionally, it has been shown that increases in water concentration, produce higher nucleation rates, which result in a decrease in average particle [18-21].

3.2. Characterization.

In Figure 4 it is shown the diffraction pattern of the synthesized solid. It can be seen the characteristic powder diffraction pattern of anatase TiO₂ in tetragonal system (PDF 00-021-0451) with a strong (011) reflection. The final Rietveld Refinement with the corrected model gave figures of merit: $R_p = 12.1$, $R_{wp} = 14.3$, $R_{exp} = 11.1$, $R_F^2 = 4.18$ (27 reflections) and $\chi^2 = 1.67$. Figure 1 shows the final Rietveld plot. The final parameters for tetragonal cell were $a = 3.7788(8)$ Å, $c = 9.4886(8)$ Å, with space group $I4_1/amd$.

The Scherrer's equation was used to estimate the particle size by averaging the value of FWHM for the first nine lines of the

powder pattern of anatase (see Table 1). Thus, the average particle size estimated for the anatase synthesized in this work was 11 nm.

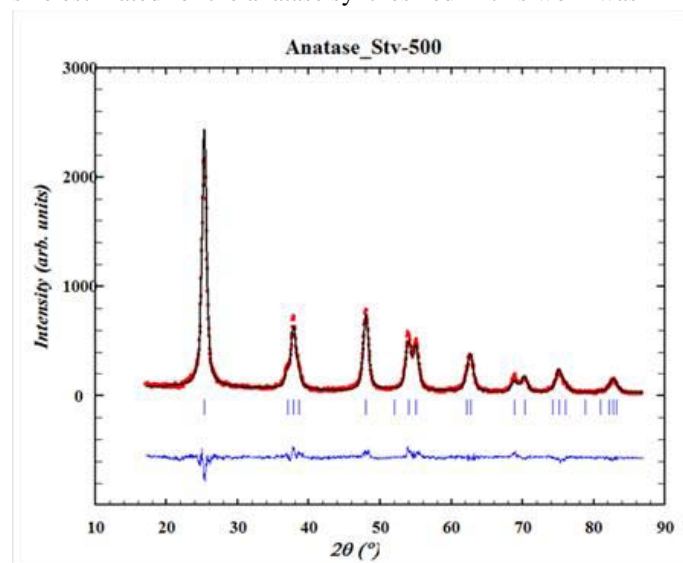


Figure 4. Final Rietveld plot for TiO₂ nanoparticles. The continuous black line represents the calculated pattern and the red dots line is the observed pattern. The blue vertical lines represent the Bragg's peaks position.

Table 1. Selected peaks employed to calculate the particles size with Scherrer's equation. These are the nine first peaks that appear in the powder pattern of TiO₂ synthesized.

<i>hkl</i>	$2\theta/^\circ$	$d_{hkl}/\text{Å}$	Int./U.A.	FWHM/ $2\theta^\circ$
101	25.313	3.515672	2432.1	0.763879
103	36.998	2.42778	136.2	0.808748
004	37.876	2.373507	593.3	0.812841
112	38.589	2.331252	105.6	0.816245
200	48.04	1.892362	797.3	0.868036
105	53.984	1.697186	492.7	0.907345
211	55.069	1.666307	465.8	0.915114

The FE-SEM and TEM studies, displayed in Figures 5-7, allow us to verify the formation of TiO₂ structures with porous tubular morphology and nanoparticles. Figures 5 and 6 show the low and high magnification FE-SEM images of the synthesized sample and confirm that the observed structures consist of aggregates of nanoparticles (Figure 5) with an average diameter of about 3-8 nm.

Conclusively, we can say that the supramolecular self-assembly of diterpene glycosides as a soft-template patterning and formation of complex system of interactions with the inorganic precursor induce the resulting morphology and the formation of pores [24].

The formation of this supramolecular soft-template has been described previously according to the theory of microphase separation. This theory was developed previously for block-copolymer and liquid crystal systems [15, 25-27].

Figures 8-10 show a high-resolution image of synthesized nanoparticles and the corresponding FFT power spectrum calculated from the region around the nanoparticles. The corresponding HRTEM image reveals that a high crystallinity exist in the mesoporous TiO₂ anatase. In Figure 8 and 9, HRTEM analysis shows lattice fringes with an interlayer distance of 0.350 nm which is close to the 0.351-0.353 nm lattice spacing of

the {101} crystal planes of the anatase TiO₂ phase, further confirmed by fast Fourier transformation (FFT) patterns, also in accordance with XRD results.

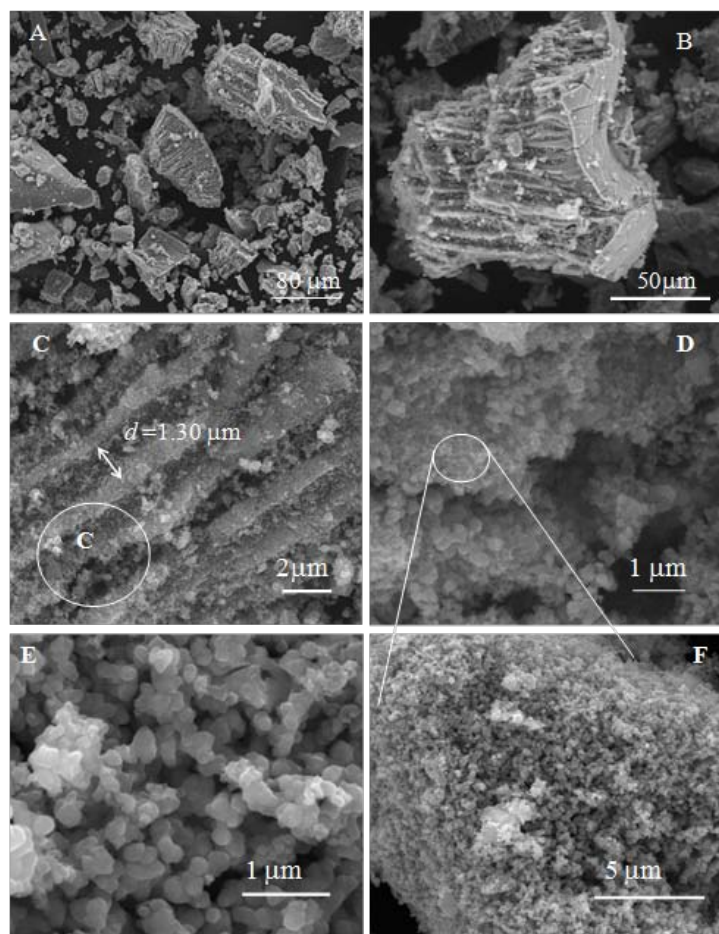


Figure 5. Images FE-SEM of synthesized anatase TiO₂ structures and nanoparticles.

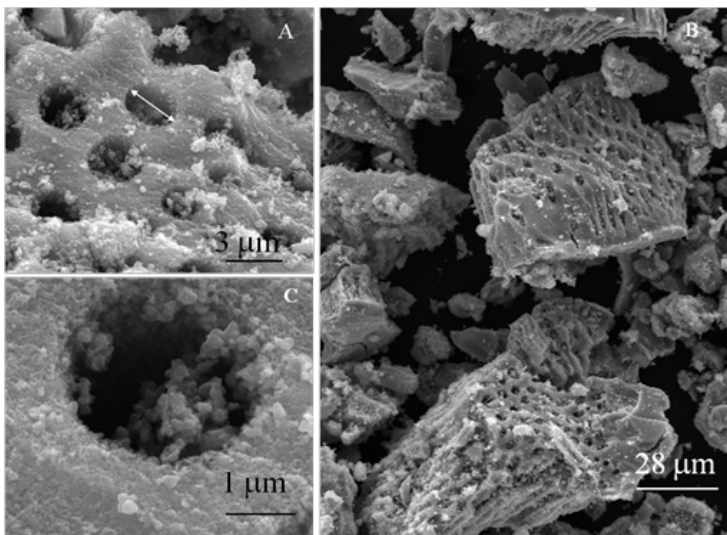


Figure 6. Images FE-SEM of synthesized anatase TiO₂ structures.

No other lattice fringes in the whole HRTEM analysis were detected. Convincingly, the obtaining of a calcined pure single-phase anatase powder nanocrystalline is confirmed. The {101} planes are the most thermodynamically stable ones for the regular anatase TiO₂ and these planes account for the 94% of the total surface according to the Wuff construction [28].

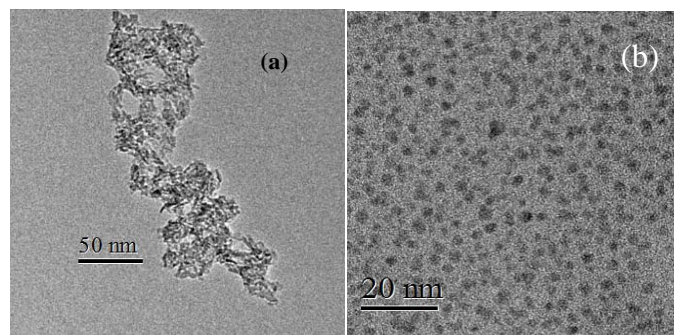


Figure 7. Images TEM of synthesized anatase TiO₂ structures (a) and nanoparticles (b).

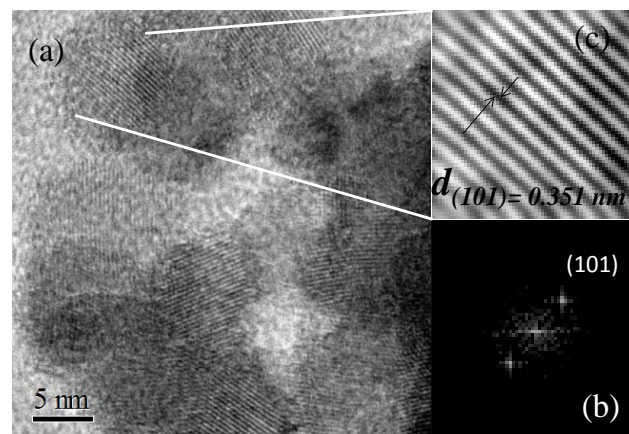


Figure 8. HRTEM image of the anatase nanoparticles (a), the corresponding FFT power spectrum (b) and resulting image after performing an inverse FFT on the masked power spectrum (c).

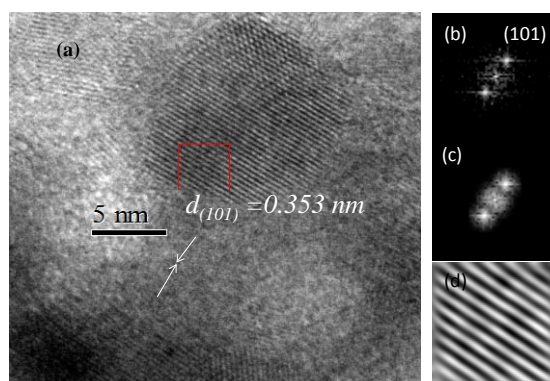


Figure 9. High magnification HRTEM Image of the anatase nanoparticles (a) and the corresponding FFT power spectrum (b) the masked power spectrum (c), resulting image after performing an inverse FFT on the masked powerspectrum (d). }

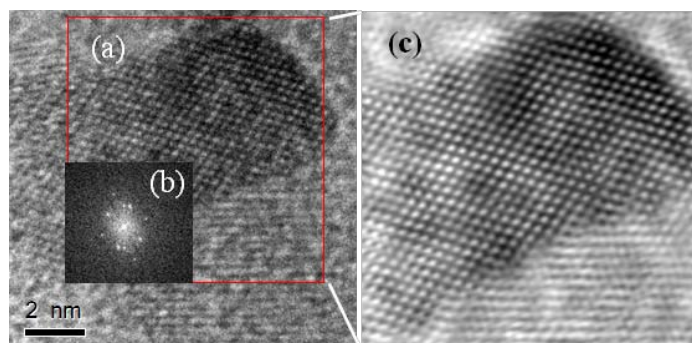


Figure 10. High magnification HRTEM Image of the porous anatase nanoparticles (a), the corresponding FFT power spectrum (b), resulting image after performing an inverse FFT on the masked power spectrum (c).

In Figures 8-10 it is demonstrated that the TiO₂ nanocrystallites have a diameter of 3–8 nm. Interestingly, Figure 10 shows HRTEM image of the TiO₂ anatase illustrating a mesoporous ordered structure.

For these studies, noise reduction was performed on a square-labeled area of the figure; a masking was applied to the intense spots of the FFT power spectrum and the resulting image after performing inverse FFT on the masked power spectrum was obtained.

In addition, physisorption of nitrogen (Figure 11), verified that the synthesized material has a surface area in the order of 258 m².g [29], which exceeds the area of an oxide of titanium commercial (51 m².g⁻¹, TiO₂ Degussa P-25). The results are consistent with the observations by TEM, allowing to demonstrate the high porosity of the materials obtained.

The characteristics of the nanomaterials make this a potentially useful material for many applications in nanotechnology, electronics, optics, catalysis, photocatalysis and other fields.

4. CONCLUSIONS

The electronic microscopy characterization (FE-SEM, TEM and HRTEM) of anatase TiO₂ powders synthesized employing *ent-Kaurane diterpenoid* glycoside molecules, as soft-templates, reveals that using this method it is possible to obtain a mesoporous material with high surface area and crystallinity. It was shown that the supramolecular arrangement that forms the *ent-Kaurane diterpenoid* serve as mold, around which a

5. REFERENCES

- [1] Danish R., Ahmed F., Koon B., Rapid synthesis of high surface area anatase titanium oxide quantum dots, *Ceram. Int.*, 40, 12675-12680, **2014**.
- [2] Pottier A., Cassaignon S., Chanéac C., Villain F., Tronc E., Jolivet J P., Size tailoring of TiO₂anatase nanoparticles in aqueous medium and synthesis of nanocomposites. Characterization by Raman spectroscopy, *J. Mater.Chem.*, 13, 877-882, **2003**.
- [3] Reyes-Coronado D., Rodriguez-Gattorno G., Espinosa-Pesqueira M. E., Cab C., Coss R., Oskam G., Phase-pure TiO₂ nanoparticles: anatase, brookite and rutile, *Nanotechnology*, 19,145605-145615, **2008**.
- [4] Li W., Zeng T., Preparation of TiO₂anatase nanocrystals by TiCl₄ hydrolysis with additive H₂SO₄, *Rev. Acad. Colomb. Cienc.*, 6,1-6, **2011**.
- [5] Sayilkan F., Asilturk M., Sayilkan H., Onal Y., Akarsu M., Arpac E., Characterization of TiO₂ synthesized in alcohol by a sol-gel process: the effects of annealing temperature and acid catalyst, *Turk. J. Chem.*, 29, 697-706, **2005**.
- [6] Klein C., Hurlbut C. S., *Manual of Mineralogy*, Twenty-First Edition, John Wiley & Sons , INC New York, **1977**.
- [7]. Park S-J., Kang Y., Park J., Evans E., Ramsier R., Chase G., Physical characteristics of titaniananofibers synthesized by Sol-Gel and Electrospinning Techniques, *J. Eng. Fiber.Fabr.*, 5, 1,50-56, **2010**.
- [8] Chen J., Hua Z., Yan Y., ZakhidovAnvar A., Baughman Ray H., XuLianbin., Template synthesis of ordered arrays of mesoporous titania spheres, *Chem. Commun.*, 46, 1872-1874, **2010**.
- [9] Bagheri S., Shameli K., Bee S., Hamid A., Synthesis and Characterization of anatase titanium dioxide nanoparticles using egg white solution via sol-gel method, *J. Chem.*, ID 848205, doi:10.1155/2013/848205, **2013**.
- [10] Ramimoghadam D., Bagheri S., Abd Hamid S.B., Biotemplated synthesis of anatase titanium dioxide nanoparticles via lignocellulosic waste material, *Biomed. Res. Int.*, ID 205636, doi:10.1155/2014/205636, **2014**.

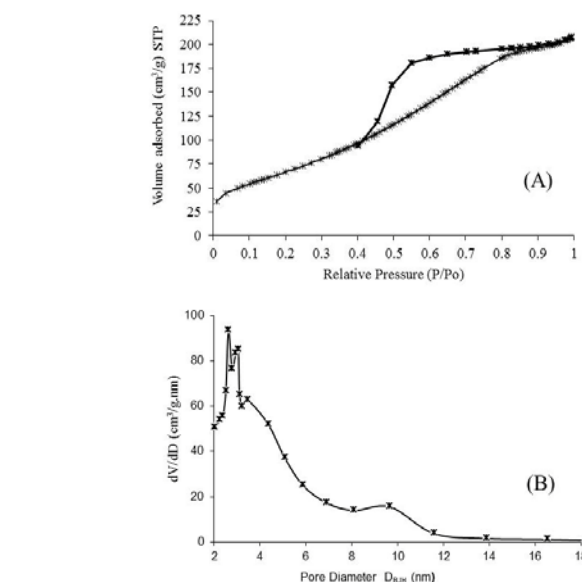


Figure 11. Nitrogen adsorption–desorption isotherm (A) and pore size distribution calculated from the desorption branch of the mesoporous TiO₂ B).

framework can be built up. The use of a titanium alkoxide as a precursor source facilitates the obtaining of structures with tubular morphology and nanoparticles with an average diameter of 3-8 nm. Protocol synthesis employed using biological materials avoids the disadvantages, which usually are present with the use of surfactants molecules, additionally it is simple and inexpensive.

- [11] An-Hui L., Dongyuan Z., Ying W., Nanocasting. *A versatile strategy for creating nanostructured porous materials*. Royal Society of Chemistry (RSC) Publishing. Nanoscience and Nanotechnology. Cambridge, CB4 0WF, UK, **2009**.
- [12] Pal N., Bhaumik A., Soft templating strategies for the synthesis of mesoporous materials: inorganic-organic, inorganic hybrid and purely organic solids, *Adv. Colloid Interface Sci.*, 189, 21-41, **2013**.
- [13] Castro A.L., Nunes M.R., Carvalho A.P., Costa F.M., Florencio M.H., Synthesis of anatase TiO₂ nanoparticles with high temperature stability and photocatalytic activity, *Solid State Sci.*, 10, 602-606, **2008**.
- [14] MuhdJulkapli N., Bagheri S., Abd Hamid S. B., Recent advances in heterogeneous photocatalytic decolorization of synthetic dyes, *The Scientific World Journal*, ID 692307, doi:10.1155/2014/692307, **2014**.
- [15] Sifontes A., Rodriguez M., Freire D., Rondón W., Llovera L., Cañizales E., Méndez F., Monaco A., Díaz Y., Biological template based on ent-kauranediterpenoid glycosides for the synthesis of inorganic porous materials, *Adv. Chem. Engineer. Sci.*, 3, 278-285, **2013**.
- [16] Nishiyama, P., Álvarez, M., Vieira, L.G., Quantitative analysis of stevioside in the leaves *Stevia rebaudiana* by near infrared reflectance spectroscopy, *J. Sci. Food Agric.*, 59, 277-281, **1992**.
- [17] Rietveld, H.M., Profile Refinement Method for Nuclear and Magnetic Structures, *J. Appl. Cryst.*, 2, 65-71, **1969**.
- [18] Simonsen M.E., Søggaard Erik G., Sol-gel reactions of titanium alkoxides and water: influence of pH and alkoxy group on cluster formation and properties of the resulting products, *J. Sol-Gel Sci. Technol.*, 53, 485-497, **2010**.
- [19] Yoldas B., Hydrolysis of titanium alkoxide and effects of hydrolytic polycondensation parameters, *J. Mater. Sci.*, 21, 1087-1092, **1986**.
- [20] Sanchez C., Livage J., Henry M., Babonneau F., Chemical Modification of Alkoxide Precursors, *J. Non-Cryst. Solids.*, 100, 65-76, **1988**.

[21] Mahshid S., Askari M., SasaniGhamsari M., Synthesis of TiO₂ nanoparticles by hydrolysis and peptization of titanium isopropoxide solution, *J. Mater. Process. Technol.*, 189, 296-300, **2007**.

[22] Barlier V., Bounor-Legare V., Boiteux G., Davenas J., Hydrolysis–condensation reactions of titanium alkoxides in thin films: A study of the steric hindrance effect by X-ray photoelectron spectroscopy, *Appl. Surf. Sci.*, 254, 5408-5412, **2008**.

[23] Doeuff S., Henry M., Sanchez C., Livage J, Hydrolysis of titanium alkoxides: modification of the molecular precursor by acetic acid, *J. Non-Cryst. Solids.*, 89,206-216, **1987**.

[24] Rodríguez M., Sifontes Á. B., Méndez F. J., Díaz Y., Cañizales E., Brito J. L., “Template synthesis and characterization of mesoporous γ -Al₂O₃ hollow nanorods using stevia rebaudiana leaf aqueous extract, *Ceram. Int.*, 39, 4499-4506, **2013**.

[25] Wanka G., Hoffmann H., Ulbricht W., Phase diagrams and aggregation behavior of poly(oxyethylene)- poly(oxypropylene)-poly(oxyethylene) triblock copolymers in aqueous solutions, *Macromolecules*, 27, 4145-4159, **1994**.

[26] Alfonsov V. A., Kataev V. E., Andreeva O. V., Beskrovniy D. V., Kovyljaeva G. I., Bakaleynik G. A., Strobykina I. Y., Litvinov I. A., Kononov A. I., The reception activity of isosteviol isolated from the plant stevia rebaudiana bertoni, Materials of the *International Symposium “Molecular design and synthesis of supramolecular architectures”*, Kazan, 27, 54-59, **2002**.

[27] Gubaidullin A. T., Mamedov V. A., Litvinov I. A., Ye H., Tsuboi S., Synthesis and comparative analysis of molecular and supramolecular structures of 4,8-disubstituted 1,5-dichloro-2,6-dioxotricyclo[5.1.0.0]octanes, *Monatsh für Chemie*, 134, 1229-1240, **2003**.

[28] Lazzeri M., Vittadini A., Selloni A., Structure and energetics of stoichiometric TiO₂ anatase surfaces. *Phys. Rev. B: Condens. Matter*, 63, 155409-155418, **2001**.

[29] Rodríguez M., Sifontes Á. B., Méndez F. J., Cañizales E., Mónaco A., Tosta M. Brito J. L., *Synthesis and characterization of anatase TiO₂ nanofibers using stevia rebaudiana leaf aqueous extract*, In: A. Gayathri, Ed., *Recent Research Developments in Material Sciences*, Research Signpost, Kerala, 3, 45-58, **2013**.

6. ACKNOWLEDGEMENTS

The authors are grateful to the Instituto Venezolano de Investigaciones Científicas (IVIC) project 1077 for financial support.